

## Factors influencing microstructural evolution in nanoparticle sintered Ag die attach

S.A. Paknejad<sup>1</sup>, A. Mansourian<sup>1</sup>, Y. Noh<sup>2</sup>, K. Khtatba<sup>1</sup>, L. Van Parijs<sup>1</sup>, S.H. Mannan<sup>1</sup>

<sup>1</sup>King's College London

Physics Department, Strand, London, WC2R 2LS, UK

Tel: 44 (0) 207 8481780 Fax: 44 (0) 207 8482420 Email: samjid.mannan@kcl.ac.uk

<sup>2</sup>King's College London

Department of Informatics, Strand, London, WC2R 2LS, UK

### Abstract

The behaviour of sintered silver die attach at high temperature has been investigated. Assemblies were made by sintering a commercially available paste composed of Ag nanoparticles with zero applied pressure on the die. The morphology of the cross sectioned surface of assemblies remains stable even at temperatures of up to 400 °C. This behaviour remained consistent even inside vacuum or after acid cleaning of the free surface. In contrast, the same sintered Ag material in the interior of a joint or sintered under a glass cover slip showed rapid microstructural changes even at 300 °C. These samples were investigated using an optical microscope to analyse the changes in the microstructure after storage at 200 to 500 °C. The observations showed a 20% increase in silver grain size after only 5 h storage at 300 °C. However, in the case of a free surface, no changes were observed after 60h storage at 400 °C. These observations were combined with DSC experiments in order to suggest the cause of the difference in behaviour. The results suggest ways of stabilizing sintered silver materials so that they can be used in applications up to 400 °C without significant structural changes occurring in the material.

### 1. Introduction

The intended operating temperature for near future electronics in many applications such as oil and gas exploration, aerospace, and automotive can be as high as 300 °C. The current available die attach materials for such applications have disadvantages such as high homologous temperature or high lead content in case of high temperature solders or sharp reduction in mechanical strength in case of Solid Liquid Inter-Diffusion (SLID) bonding materials [1].

To overcome these issues, many researchers have been trying to develop a technique using sintering of nanoparticles [2-5]. In this case the small size of nanoparticles contribute to a high surface energy and therefore lower melting and sintering temperatures. For instance, 2.4 nm

silver particles have a melting point of about only 350 °C [2], which can be compared with the 961°C melting point of bulk silver. In this case as the processing temperature can be lower than the operating temperature, the issues with the homologous temperature can be avoided.

While many studies have been performed on sintering of nanoparticles [6, 7], or the general mechanical features of sintered structures [8, 9], only a small number of these studies are focused on high temperature behaviour of sintered silver at or above 300 °C [10-13]. In the present study in-situ observations of morphological changes on sintered silver have been performed. The conclusions suggest possible routes to enable sintered silver to perform in extreme high temperature applications.

## 2. Experimental

Two silver nanoparticle pastes intended for pressure-less sintering processes, NanoTach® N and NanoTach® X from NBE Tech have been used for these studies. NanoTach® N is only recommended for die sizes of up to 3×3 mm, whereas NanoTach® X is recommended for die sizes up to 10×10 mm. All the samples have been produced under zero applied pressure and by following the recommended sintering profiles.

Sample set 1, was prepared by assembling Ag backed Si die onto Ag backed Si substrates, using NanoTach® N paste. The samples were mounted using a hot mounting resin, LevoFast from Struers after the sintering, this resin being chosen because it was capable of withstanding high temperature storage. The samples were cross sectioned and mechanical polished using silicon carbide cloths followed by diamond suspensions of 3 and 0.25 µm diameter. They were then put into high temperature storage in order to track the shape evolution of individual pores and grains at the cross sectioned surface. The samples were stored at 300 °C for periods of 1, 3, 4, and 20 h. Previous studies using identical pastes and die, but with the cross-sectioning carried out only after high temperature storage indicated that significant changes in pore and grain shape should be expected [11,13].

Three other sample sets were produced using NanoTach® X paste. Sample set 2 was produced by manual paste deposition onto glass slides followed by cover-slip placement on top of the paste (substituting for die placement). The cover-slips were

produced by Menzel-Gläser with 150 µm thicknesses, and they were cut into 10×10 mm squares. These samples were then observed pre and post high temperature storage at 200, 300, 350, 400, 450, and 500 °C in air to analyse and compare the microstructural changes of constrained sintered silver under the cover-slip. Sample set 3 was prepared by stencil printing of NanoTach® X into wire shaped gaps with 150 µm thickness and width and with ~4 mm length. These samples were prepared in order to observe the changes of the microstructure on a planar free surface of sintered silver, without exposure to the cross sectioning process of sample set 1. These samples were kept at 300 and 400 °C inside 5 mPa vacuum and at 450 and 500 °C in air. The final set of samples were prepared by deposition of the paste inside custom-made glass sample holders, see Fig. 1 below. These sample holders were designed for surface cleaning of the sintered silver samples in 20% concentration perchloric acid. The newly cleaned surface was kept under deionised water for protection against atmosphere until transfer to a vacuum oven. This set was stored at 300 °C inside about 40mPa of pressure for 5 h. Table 1 lists the materials used in each sample set together with the intended experiment.

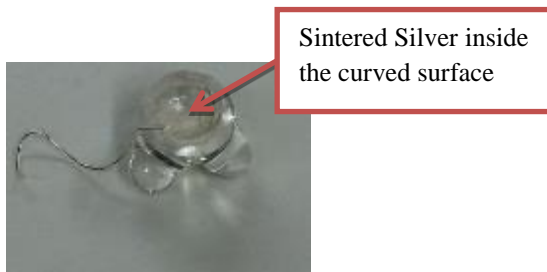


**Fig. 1.** Customized glass sample holder for surface contamination removal process and protection of the sample against atmosphere by merging under deionized water. The silver wire coming out of the sample holder has been intended for charge removal

A Hitachi S4000 Scanning Electron Microscope (SEM) was used for investigating the free surfaces of sintered silver samples. For the samples sintered under cover-slips a Zeiss Axio Lab.A1 optical microscope has been utilized. The produced images were then further analysed using the Image processing toolbox in Matlab and ImageJ 1.46r. The Samples of NanoTach® X paste both pre and post sintering were analysed using a Differential Scanning Calorimetry (DSC) (Mettler Toledo DSC822e).

**Table 1. Sample sets.**

Sample set No.	Purpose of experiment	Paste type and surface dimensions	Preparation Method
1	Free surface observation after high temperature storage once cross sectioned	NanoTach® N 2.5×2.5 mm	Recommended sintering profile after manual paste deposition and die placement
2	Constrained surface observation after high temperature storage	NanoTach® X 10×10 mm	Recommended sintering profile after manual paste deposition and cover slip placement
3	Free surface observation without cross sectioning after high temperature storage	NanoTach® X 150 $\mu\text{m}$ ×4 mm	Recommended sintering profile after stencil printing of the paste
4	Free surface observation after acid cleaning and high temperature storage	NanoTach® X $r = 2$ mm	Recommended sintering profile after paste deposition

### 3. Results and Discussions

The cross-sectioned sample, sample set 1, did not indicate any changes in the morphology of sintered silver even after overall storage of 30 h at 300 °C, vividly contrasting with previously reported observations [11-13]. The difference here was the order of procedures, in that cross sectioning was performed before aging at high

temperatures. Therefore, sample sets 2-4 have been produced to investigate whether contamination from cross-sectioning or exposure to air was the primary cause of the difference in microstructural behaviour.

Sample set 2 was produced in order to eliminate the various environmental factors that sample set 1 had been exposed to, while still



allowing in-situ observation of individual pore and grain evolution. Fig. 2 demonstrates considerable differences between pre and post high temperature storage, observed through the glass cover slip. While Fig. 2 (a) and (b) indicate no apparent change in the grain structure after

5 h storage at 200 °C, Fig 2 (c) and (d) shows considerable changes in the microstructure of sintered silver after only 5 h at 300 °C. Fig 2 (e) and (f) indicate a sharp rise in grain growth at higher temperature.

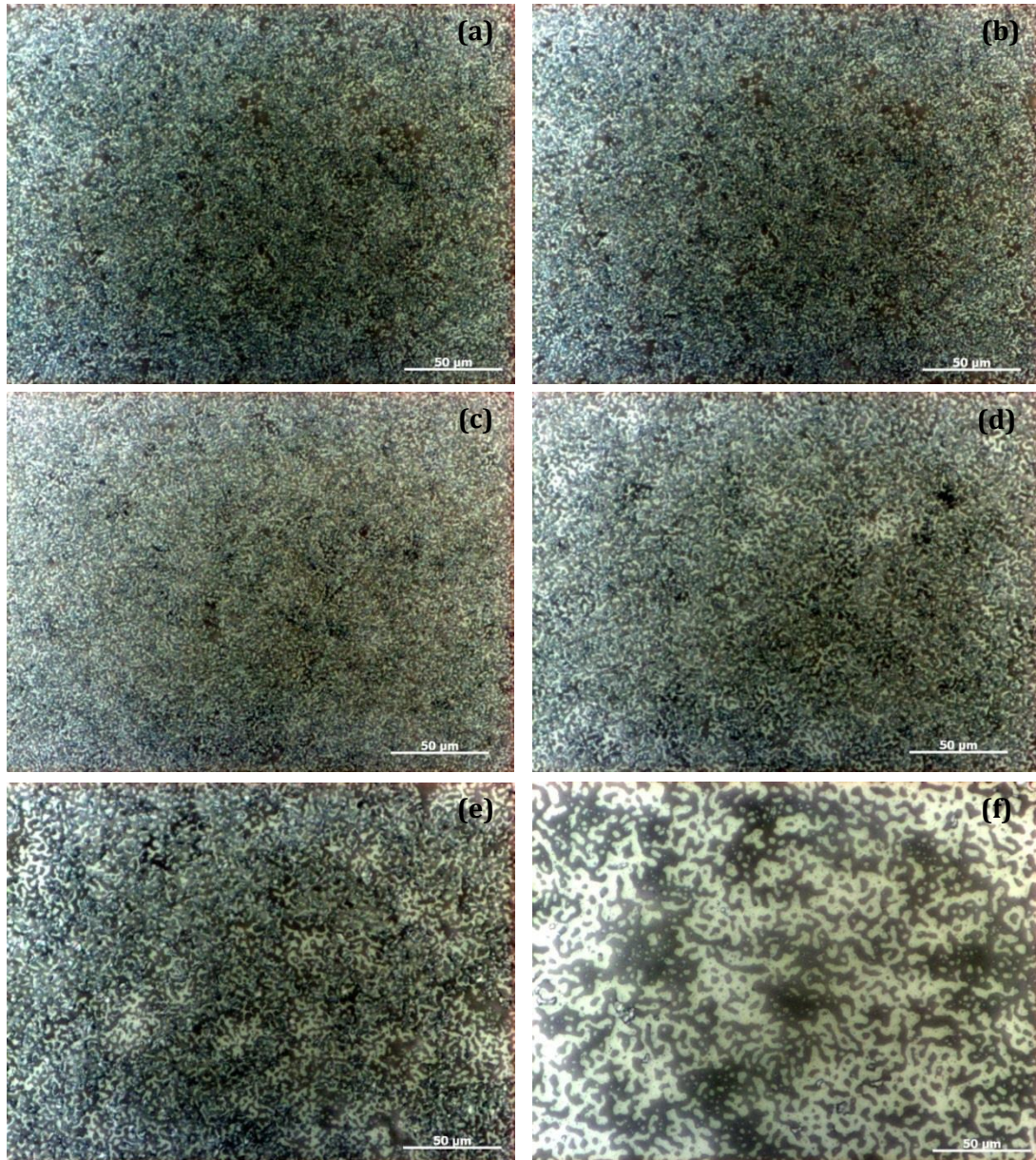


**Fig. 2.** Optical images of sintered silver under cover slip stored in air. (a) before storage at 200°C. (b) Image of same area as (a) after 200°C for 5h. (c) Image before storage at 300°C. (d) Image of same area as (c) after 300°C for 5h. (e) 400°C for 5h. (f) 500°C for 5h.



To quantitatively analyse the grain growth of sintered silver during the 5 h storage, the Matlab image processing toolbox and ImageJ software were used. Fig. 3 shows the steps taken to perform the grain size measurements on the optical images of sample set 2. The data obtained from these measurements have been plotted against temperature to compare the grain sizes after storage to their initial sizes, shown in Fig. 4. It is interesting to note that the grain growth rate increases sharply after 350 °C, and

presence of two linear sections with very different gradients suggests presence of two different grain growth mechanism at those temperature regimes. In addition, the average grain size has increased by about 20% after 5 h storage at 300 °C, which is unlike sample set 1 where no grain change was been observed even after 30 h at this temperature. Furthermore, negligible changes to the grain sizes at 200 h indicate a relatively stable structure of sintered silver up to such temperatures.

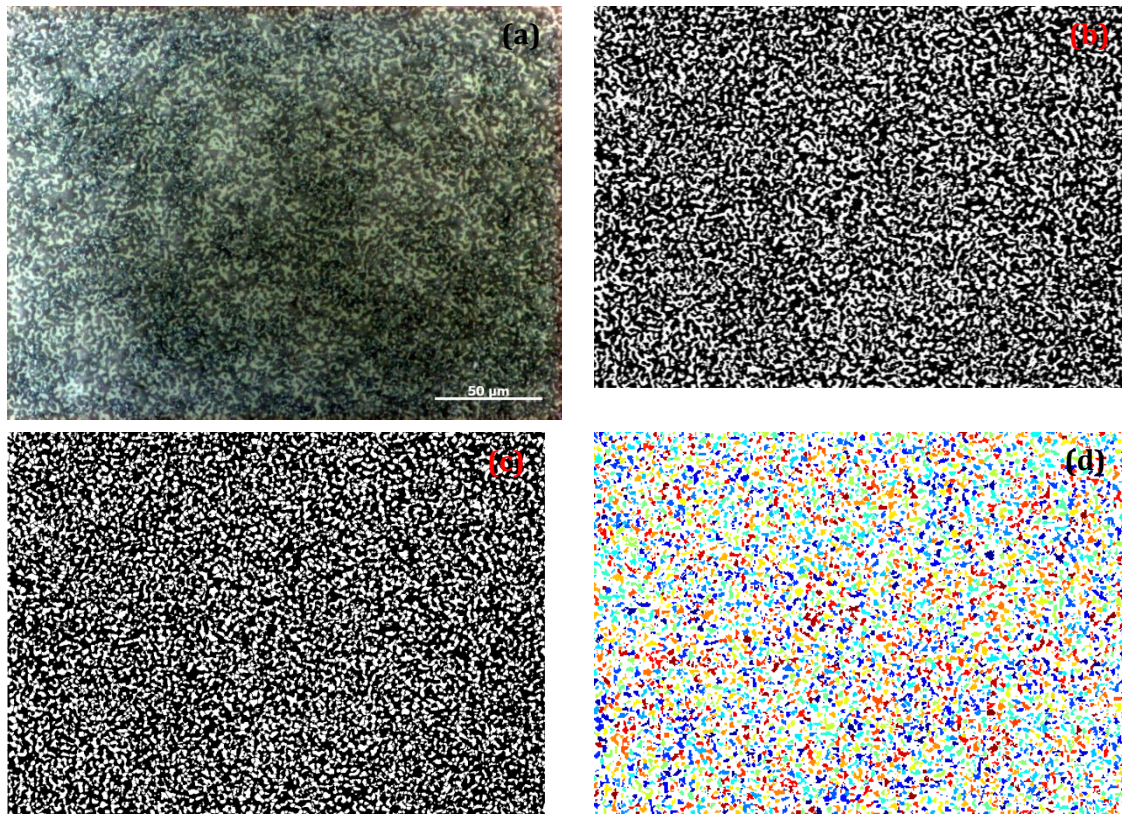


**Fig. 3.** Processing of optical images for grain size measurements. (a) Typical area on sintered silver stored at 350 °C for 5h to illustrate the technique. (b) Binary image of (a) produced in Matlab by a local thresholding technique [14] to overcome the uneven background. (c) Watershed segmentation of (b) using ImageJ. (d) Grain area and quantity calculated for estimating the average grain size using MatLab (coloured for illustration proposes).

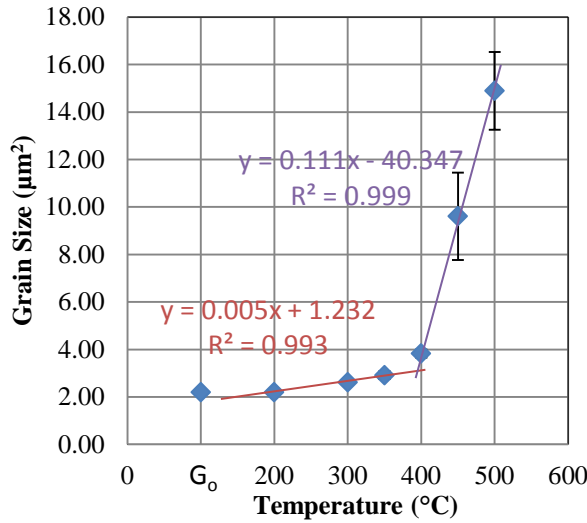


**Fig. 4.** The average grain sizes vs. storage temperature for 5h.  $G_0$  is the initial grain size after sintering.

The third set of samples eliminated the cross sectioning process by stencil

printing of the silver paste. Therefore, the only contributing factor to any microstructural behaviour difference to sample set 2 and the previously performed experiments [11-13] is exposure to atmosphere prior to aging. Fig. 5 (a) shows the free surface of the sintered silver before aging, showing that it is identical to Fig 5 (b) and (c), where the samples experienced overall aging of 40h at 300 °C and 66 h at 400 °C both in vacuum. However, additional storage at 500 °C in air for 24 h has greatly changed the structure of the sintered silver; Fig. 5 (d). Performing 300 °C aging of another sample from set 3 for 24 h in air also did not result in any changes. While 66 h at 400 °C did not produce any changes to the morphology, only half hour storage at 500 °C resulted in considerable changes; Fig. 6.

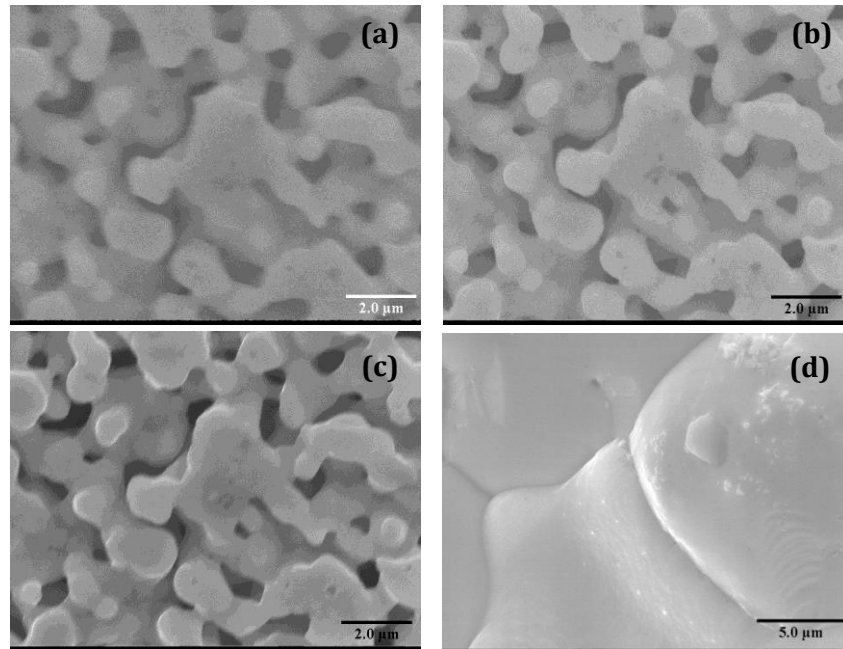


**Fig. 5.** SEM images from sample set 3 after high temperature storage in vacuum each looking at the same area of the sintered silver. (a) 0h. (b) 24h at 300°C. (c) Additional 16h at 300°C and 66h at 400°C. (d) Additional 24h at 500°C (not in vacuum, and the original area was not identified).

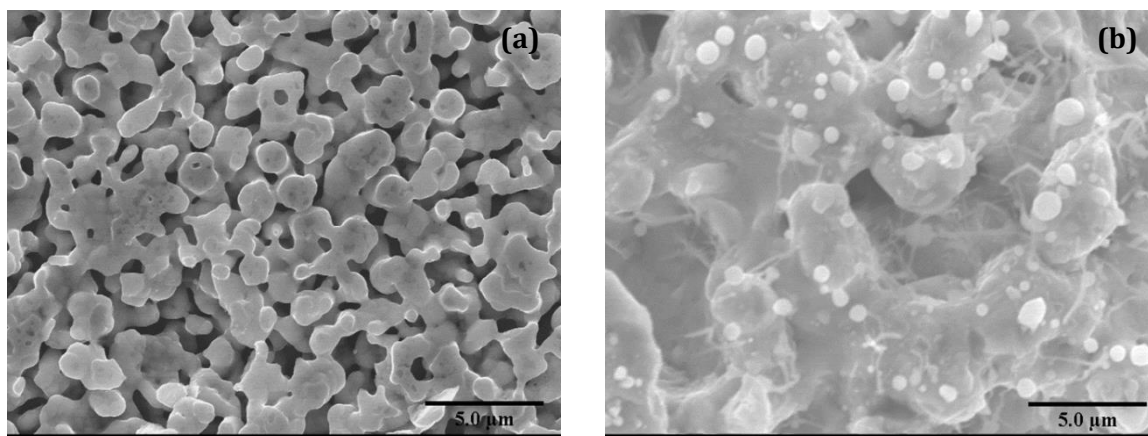


**Fig. 6.** SEM image of high temperature storage at 500°C in air. (a) 0h. (b) 0.5h (original area was not identified).

These observations point out to the presence of a passivating material on the surface of the sintered silver, which appears to prevent the surface diffusion of atoms on their free surfaces. As a result of the arrest of surface diffusion, the expected changes to the microstructure are also halted. DSC experiments on NanoTach® X show the presence of an exothermic and irreversible peak at around 450 °C, (see Fig. 7), which appears to confirm the decomposition of the surface passivating material. Further observations on the high temperature behaviour of sintered silver from sample set 3 have shown interesting results. As shown in Fig. 8, storage at 450 °C for 1 h in air did not result in any observable changes to the structure, while an additional 1.5 h completely changed the structure. This again seems to be resulted by the passivating layer, which requires the initial 1 h period to decompose and enable surface diffusion and consequently grain evolution. To further investigate the passivating layer, sample set

4 has been stored inside perchloric solution for 30 min and after cleaning, stored under deionised water for further protection. However, after placement of the sample inside 300 °C for 5 h no change has been observed indicating the possibility of nonorganic background of the passivating layer.

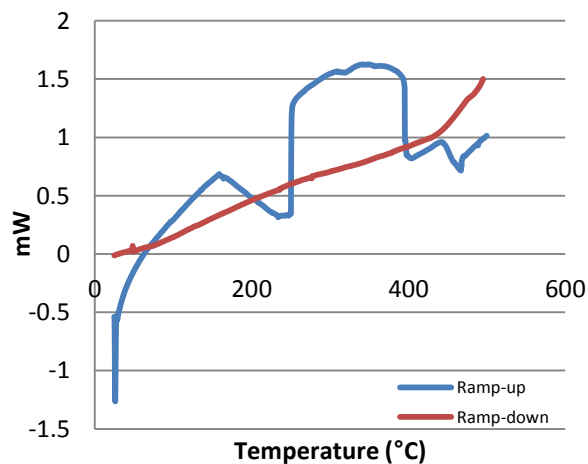


**Fig. 7.** DSC of sintered silver. Ramp rate 10 °C/min and sample weight 10.5 mg.



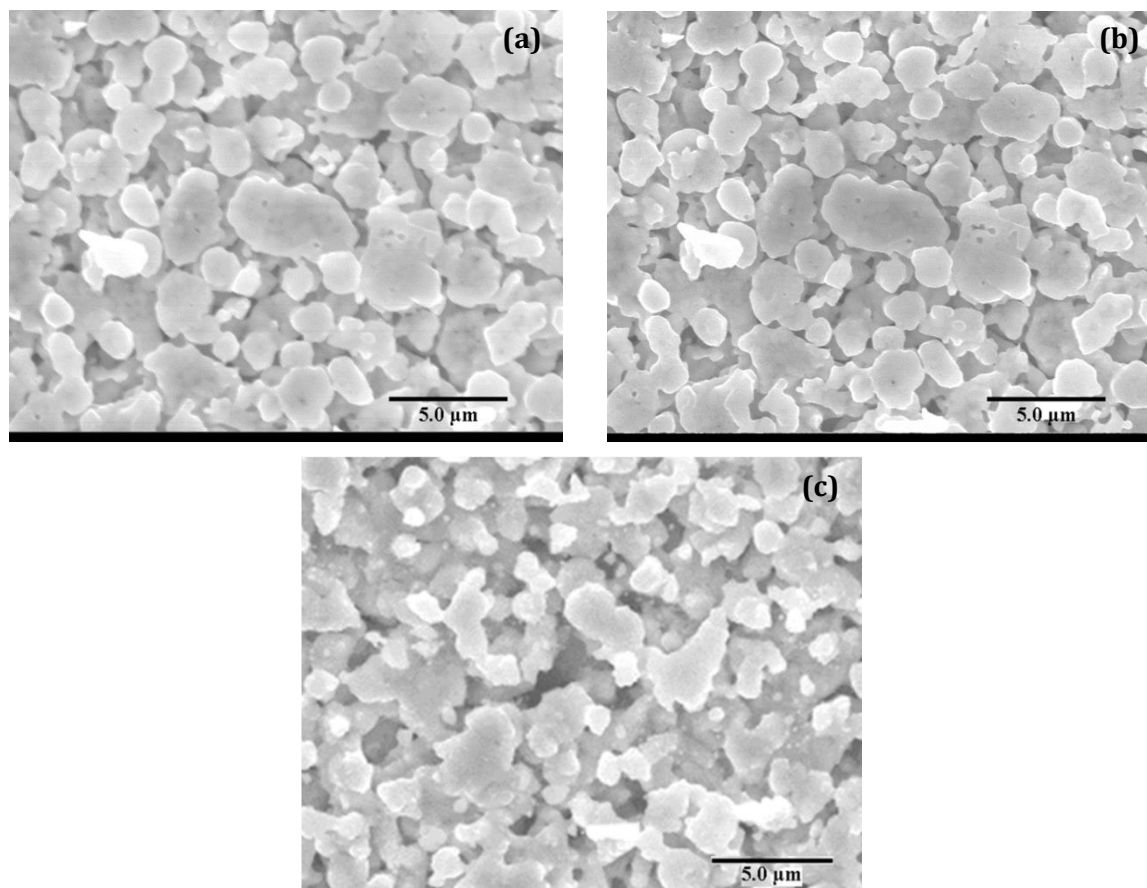


**Fig. 8.** SEM images of high temperature storage at 450°C in air. (a) 0h. (b) 1h (c) Additional 1.5h.

#### 4. Conclusions

It has been observed that exposure to atmosphere of sintered silver can stop the surface diffusion of atoms and result in preservation of the initial structure even at 400 °C. However, the surface of sintered silver protected by cover-slip has greatly changed during storage at 300 °C. Therefore, if the passivation layer could be formed on the interior sintered silver pore surfaces, e.g. by altering the chemical composition of the paste, it may stabilize the microstructure and result in die attach materials with longer lifetimes at high temperatures than current systems.

It has also been noted that the microstructural evolution of sintered silver without the passivation layer increases gradually from 200 °C to 350 °C, but from 400 °C to 500

°C the changes happen much more rapidly. In addition, the microstructure on the free surface of sintered silver evolves after a delay of more than 1 h at 450 °C, which can be attributed to the time required for removal of the passivation layer. Furthermore, the acid cleaning procedure indicates that the passivation layer is unlikely to be composed of organic compounds, and is more likely to be one of the silver oxides which can form.

For future work, it is recommended to perform XPS on the free surface of sintered silver to fully determine the composition of the passivating layer.



## Acknowledgements

The author would like to thank Messrs. G. Lewis and G. Dumas from Eltek Semiconductors Ltd for supply of materials and Messrs J. Greenberg, E. Samuel and W. Luckhurst for their help during the experimental procedures.

## References

- [1] T. Tollefsen, O. Løvvik, K. Aasmundtveit, A. Larsson, Metallurgical and Materials Transactions A, 44 (2013) 2914-2916.
- [2] M. Maruyama, R. Matsubayashi, H. Iwakuro, S. Isoda, T. Komatsu, Applied Physics A, 93 (2008) 467-470.
- [3] Y. Akada, H. Tatsumi, T. Yamaguchi, A. Hirose, T. Morita, E. Ide, Materials transactions, 49 (2008) 1537-1545.
- [4] J.G. Bai, G.-Q. Lu, Device and Materials Reliability, IEEE Transactions on, 6 (2006) 436-441.
- [5] K.S. Siow, Journal of alloys and compounds, 514 (2012) 6-19.
- [6] K. Nakaso, M. Shimada, K. Okuyama, K. Deppert, Journal of Aerosol Science, 33 (2002) 1061-1074.
- [7] A. Moitra, S. Kim, S.-G. Kim, S.J. Park, R.M. German, M.F. Horstemeyer, Acta Materialia, 58 (2010) 3939-3951.
- [8] E. Ide, S. Angata, A. Hirose, K.F. Kobayashi, Acta Materialia, 53 (2005) 2385-2393.
- [9] P. Peng, A. Hu, B. Zhao, A.P. Gerlich, Y.N. Zhou, Journal of Materials Science, 47 (2012) 6801-6811.
- [10] W. Leong Ching, S. Wen Wei, E.P.J. Rong, D. Mian Zhi, V.S. Rao, D.R. MinWoo, Electronics Packaging Technology Conference (EPTC 2013), 2013 IEEE 15th, 2013, pp. 335-340.
- [11] G.D. G. Lewis, and S. H. Mannan, HiTEN 2013, IMAPS Oxford, 2013, pp. 237 – 245.
- [12] F. Yu, R.W. Johnson, M. Hamilton, HiTEC 2014, IMAPS, Albuquerque, 2014.
- [13] S. Paknejad, G. Dumas, G. West, G. Lewis, S. Mannan, Journal of Alloys and Compounds, 617 (2014) 994-1001.
- [14] B. Shoelson, ThresholdLocally. Accessed on 13/04/2015 from <http://www.mathworks.com/matlabcentral/fileexchange/29764-thresholdlocally>, last update 08/02/2011.